CHEMICAL ENGINEERING TRANSACTIONS
VOL. 62, 2017
A publication of AIDIC
The Italian Association of Chemical Engineering
Online at www.aidic.it/cet
Guest Editors: Fei Song, Haibo Wang, Fang He

ISBN 978-88-95608- 60-0; **ISSN** 2283-9216
DOI: 10.3303/CET1762151

Modeling and Characterization of Mechanically Mediated Structure of Terfenol-D, Pb(Zr, Ti)O_3 and Nonmagnetic Flakes

Xiangyang Li[a,b], Jing Liu*[a,c], Weipeng Zhang[a]

[a]School of Mechanical and Electronic Engineering, Ningbo Dahongying University, Ningbo 315175, China
[b]Magnetoelectronic Laboratory, Nanjing Normal University, Nanjing 210023, China
[c]Piezoelectric Device Laboratory, Ningbo University, Ningbo 315211, China
liujing@nbdhyu.edu.cn

The magnetoelectric samples studied were made up of Terfenol-D, Pb(Zr,Ti)O3 and nonmagnetic flakes. The magnetic-mechanical-electric transform originating from the magnetostrictive effect of Terfenol-D caused the magnetoelectric coupling. The measured results indicated a strong dependence of the magnetoelectric voltage coefficient (α_v) on the DC bias magnetic field (H_{dc}). One or two peaks could be observed in the α_v-H_{dc} curve at a resonance frequency, which was attributed to two piezomagnetic coefficient components for Terfenol-D. The dependence of the peak voltage on H_{dc} was investigated, indicating that the piezomagnetic coefficient was the cause. By taking advantage of these performances, this paper used magnetoelectric materials to make the sensor for low AC magnetic field detection.

1. Introduction

Magnetoelectric (Hereinafter referred to as ME) materials have intrigued tremendous interests due to their wide applications to ME devices, such as ME sensors, actuators and transducers (Liu et al., 2017; Wu et al., 2011). Taking the advantage of products using magnetostrictive and piezoelectric effects, the ME coupling could be realized in a composite consisting of ferroelectric and ferromagnetic phases (Li et al., 2013; Bi et al., 2010). The realization of layered ME composites has been a considerable progress in the study of the ME effect in recent years, as the mechanical deformation of the magnetostrictive layer was coupled with the piezoelectric layer through adhesive layer under an applied magnetic field and an enhanced electric polarization was generated (Nan et al., 2008). However, layered ME composites were not easy for application because there was actually no ideal interface coupling properties (Zeng et al., 2010).
Reports about ME coupling realization by acoustic wave guide suggested that more ME materials could be obtained as long as the magnetic force was coupled to the piezoelectric phase (Li et al., 2016; Bi et al., 2011). This paper reported two ME structures made up of several magnetostrictive flakes, piezoelectric flakes and nonmagnetic flakes according to the idea. Improved stretching stress coupling has been observed among one and two magnetostrictive flakes samples. Interestingly, the treads of ME voltage coefficient depending on H_{dc} in these two kinds of construction were entirely different.

2. Experiments

The ME structure of MPM was consisted of two magnetostrictive Terfenol-D flakes, a piezoelectric PZT flake and two nonmagnetic (glass) flakes, as shown in Figure 1(a) where PZT and Terfenol-D were used as the piezoelectric and magnetostrictive phases respectively. The schema of the prepared structure of PMP was shown in Figure 1(b), where the commercial PZT flake was poled in the direction of thickness and cut with dimensions of 14×6×1.2 mm^3 (l×w×t) . Two commercial Terfenol-D flakes were prepared with dimensions of 14×6×0.6 mm^3, and thus the total thickness of Terfenol-D was equal to PZT. As for PMP sample, the dimensions of PZT flakes and Terfenol-D flake were 14×6×0.6 mm^3 and 14×6×1.2 mm^3. We could find that the volume fractions of PZT and Terfenol-D for PMP and MPM were equal. The piezoelectric and magnetostrictive flakes were placed parallel to the longitudinal direction, and then bonded to two glass slides with a slow-dry epoxy to form an end bonding structure.

Please cite this article as: Xiangyang Li, Jing Liu, Weipeng Zhang, 2017, Modeling and characterization of mechanically mediated structure of terfenol-d, pb(zr, ti)o3 and nonmagnetic flakes, Chemical Engineering Transactions, 62, 901-906 DOI:10.3303/CET1762151

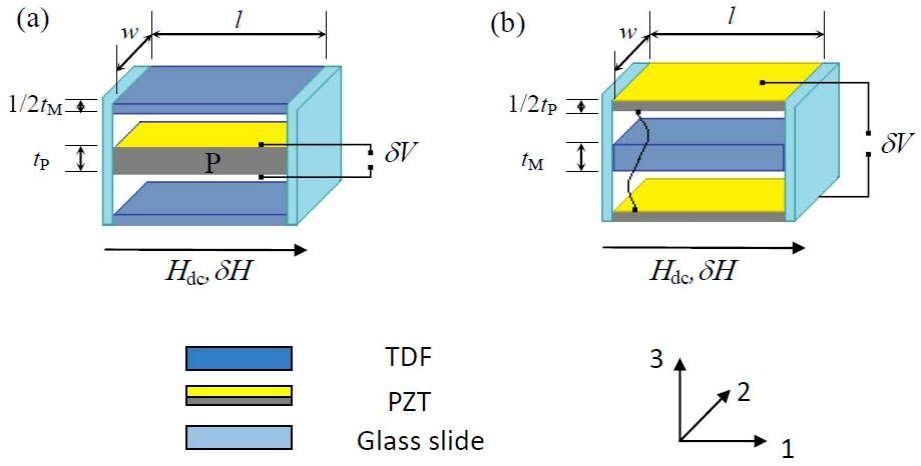

Figure 1: (a) Schematic diagram of the proposed structure of MPM, (b) Schematic diagram of the proposed structure of PMP.

By taking MPM as an example, the sample was placed in a Helmholtz coil and applied to a small AC magnetic field (H_{dc}) with the peak 1 Oe value along the longitudinal direction of the Terfenol-D flakes, and a bias magnetic field (H_{dc}) generated by an electromagnet was superimposed to H_{dc} along the same direction. Deformation emerged in magnetostrictive flakes as a result of the magnetostrictive effect, and what producing the stretching stress in PZT flake as the end parts of Terfenol-D and PZT flakes were inseparably linked. The voltages induced across the PZT flake due to the piezoelectric effect, and then they were measured for various H_{dc} and H_{ac} over a wide frequency range of 1–150 kHz by using a lock-in amplifier method. The ME voltage coefficient was calculated by using the formula $\alpha_v=\delta V/(\delta H \cdot t_P)$, where t_P was the total thickness of PZT.

3. Results and Discussion

Figure 2(a) shows the measured α_v as a function of AC magnetic field frequency for PMP in various bias magnetic fields. First, the fundamental mode resonance of the PMP was found to be approximately 81 kHz, and a sharp resonance peak was observed for H_{dc} = 25, 800 and 1500 Oe in the applied frequency range. Second, the peak value increased as the H_{dc} increased from 25 Oe to 1500 Oe, and the maximum α_v reached 5.0 (V/cm Oe).

As is known to all, the ME coupling effect can be enhanced under the electromechanical and ferromagnetic resonances. As a transducer, the structure can be approximated to layered ME composites, and the resonance frequency of the planar acoustic resonance mode can be written as:

$$f_{r1} = \frac{1}{2l}\sqrt{\frac{1}{\bar{\rho}\overline{s_{11}}}} \tag{1}$$

where l was the length of the Terfenol-D flake, and $\bar{\rho}$ was the average density calculated by $\bar{\rho}=v_E\rho_E+ v_H\rho_H$, where ρ_E and ρ_H were the density while v_E and v_H were the volume fractions of the PZT and Terfenol-D flakes respectively. The equivalent elastic compliance value $\overline{S_{11}}$ should be written as:

$$\overline{s_{11}} = \frac{s_{11}^E s_{33}^H}{v_E s_{33}^H + v_H s_{11}^E} \tag{2}$$

Taking ρ_E=7.7×10^3 kg m^{-3}, ρ_H=9.2×10^3 kg m^{-3}, *SE 11*=15.9×10^{-12} m^2 N^{-1}, *S33 H*=40×10^{-12} m^2 N^{-1} and collecting Eqs. (1) and (2), it can be predicted that the planar acoustic resonance frequency is 81.5kHz. As can be seen in Fig. 2(a), the resonance frequencies of PMP were 81.8, 80.8 and 81.1KHz for H_{dc} = 25, 800 and 1500Oe, the calculated values were very close to the measured ones.

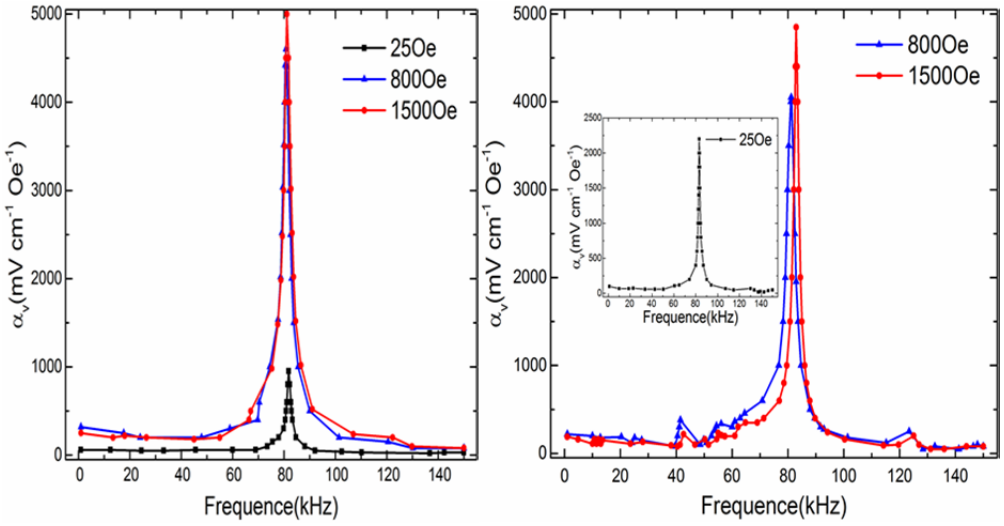

(a) (b)

Figure 2: (a) Magnetoelectric voltage coefficient as a function of frequency for PMP, (b) Magnetoelectric voltage coefficient as a function of frequency for MPM, and the inset shows the magnetoelectric voltage coefficient as a function of frequency at H_{dc} = 25 Oe.

As shown in Figure 2(b), the position of the resonance peak moved with H_{dc} increasing from 0 Oe to 1500 Oe, which was not found in the PMP structure studies. This indicated the possibility of using PMP and MPM structure for DC magnetic field detection (Lei and Wang, 2014). The dependence of ME voltage coefficient on H_{dc} for MPM was very different from that for PMP, and here three resonance peaks were observed for H_{dc}= 800 and 1500 Oe. The bending-mode resonant frequency was given by (Wan et al., 2005):

$$f_{r2} = \frac{\pi d}{4\sqrt{3}l^2}\sqrt{\frac{1}{\rho \overline{\overline{s}}_{11}}}\left(n+\frac{1}{2}\right)^2 \tag{3}$$

where *n* was the order of bending resonant mode, and *d* was the thickness of PZT flake. Calculated by the typical material parameters above, the second, third and forth bending resonance frequencies were 39.7, 77.9, and 128.7 kHz. As can be seen, the calculated values were in agreement with the frequencies observed in Figure 2(b), suggesting that the theoretical model discussed above was believable and the resonance peaks could be attributed to the bending resonance mode.

Figure 3(a) shows α_v at resonance frequency 81 kHz as a function of H_{dc} for MPM and PMP. With the increasing H_{dc} up to 1600 Oe, the ME voltage coefficient for PMP first increased rapidly and then decreased smoothly, which could be related to the piezomagnetic coefficient of magnetostrictive phase (Liu et al., 2003). The piezomagnetic coefficient could be deduced according to the Z-L constitutive model of magnetostrictive phase, and the Taylor expansion of the Gibbs free energy *G(σ, M)* in the neighborhood of point *(σ, M)=(0, 0)* could be written in the form as:

$$\begin{aligned} G(\sigma,M) = {} & \frac{1}{2}\frac{\partial^2 G}{\partial\sigma^2}\sigma^2 + \frac{1}{3!}\frac{\partial^3 G}{\partial\sigma^3}\sigma^3 + \frac{1}{4!}\frac{\partial^4 G}{\partial\sigma^4}\sigma^4 + \ldots + \frac{3}{3!}\frac{\partial^3 G}{\partial\sigma\partial M^2}\sigma M^2 + \\ & \frac{6}{4!}\frac{\partial^3 G}{\partial\sigma^2\partial M^2}\sigma^2 M^2 + \ldots + \frac{1}{2}\frac{\partial^2 G}{\partial M^2}M^2 + \frac{1}{4!}\frac{\partial^4 G}{\partial M^4}M^4 + \ldots \end{aligned} \tag{4}$$

The thermodynamic equation was given by $S = -\frac{\partial G}{\partial\sigma}$ and $B = -\frac{\partial G}{\partial H}$, so we had $S = -\frac{\partial^2 G}{\partial\sigma^2}\sigma - \frac{1}{2}\frac{\partial^3 G}{\partial\sigma^3}\sigma^2 - \frac{1}{3!}\frac{\partial^4 G}{\partial\sigma^4}\sigma^3 + \cdots - \frac{1}{2}(\frac{\partial^3 G}{\partial\sigma\partial M^2} + \frac{\partial^4 G}{\partial\sigma^2\partial M^2}\sigma + \cdots)M^2$, and $\mu_0 \mathrm{H} = -\frac{\partial^2 G}{\partial\sigma^2}M + \frac{1}{3!}\frac{\partial^4 G}{\partial\sigma^4}M^3 + \cdots + (\frac{\partial^3 G}{\partial\sigma\partial M^2} + \frac{1}{2}\frac{\partial^4 G}{\partial\sigma^2\partial M^2}\sigma^2 + \cdots)M$. Based on the already known characteristics of magnetostrictive materials, the above polynomial could be represented as follows: $-\frac{\partial^2 G}{\partial\sigma^2}\sigma - \frac{1}{2}\frac{\partial^3 G}{\partial\sigma^3}\sigma^2 - \ldots = \frac{\sigma}{E_s} + \lambda_0(\sigma)$, $\frac{\lambda_0(\sigma)}{\lambda_s} = \tanh(\frac{\sigma}{\sigma_s})$, where λ_s was the saturation magnetostrictive coefficient and $\lambda_0(\sigma)$ was the nonlinear elastic strain. Therefore, the Z-L constitutive model could be derived as:

$$S = \frac{\sigma}{E_s^Y} + \lambda_0(\sigma) + \frac{\lambda_s - \lambda_0(\sigma)}{M_s^2} M^2$$
$$H = \frac{1}{\eta} f^{-1}\left(\frac{M}{M_s}\right) - \frac{2[\lambda_s \sigma - \Lambda_0(\sigma)]}{\mu_0 M_s^2} M \quad (5)$$

Where $\eta = \frac{3\chi_m}{M_s}$, χ_m is the initial magnetization coefficient, and $\Lambda_0(\sigma) = \int_0^\sigma \lambda_0(\sigma) d\sigma$.

Considering the condition $\sigma=0$, we could write $S = \frac{\lambda_s}{M_s^2} M^2$ and $\frac{M}{M^2} = \coth(\eta H) - \frac{1}{\eta H}$. While considering $\frac{\partial S}{\partial M} = 2\frac{\lambda_s}{M_s^2} M$ and $\frac{\partial M}{\partial H} = M_s(\eta(1 - \coth(\eta H)^2) + \frac{1}{\eta H^2})$, we could derive the consequence as:

$$d_{11,m} = \frac{\partial S}{\partial H} = \frac{\partial S}{\partial M}\frac{\partial M}{\partial H} = 2\lambda_s\left(\coth(\eta H) - \frac{1}{\eta H}\right)\left(\eta\left(1 - \coth(\eta H)^2 + \frac{1}{\eta H^2}\right)\right) \quad (6)$$

From Equation (6), it could be found that the $d_{11,\,m}$ for magnetostrictive phase increased and achieved a certain maximum, and then decreased with increasing H_{dc}, which were in good agreement with the observed results in Figure 3(a).

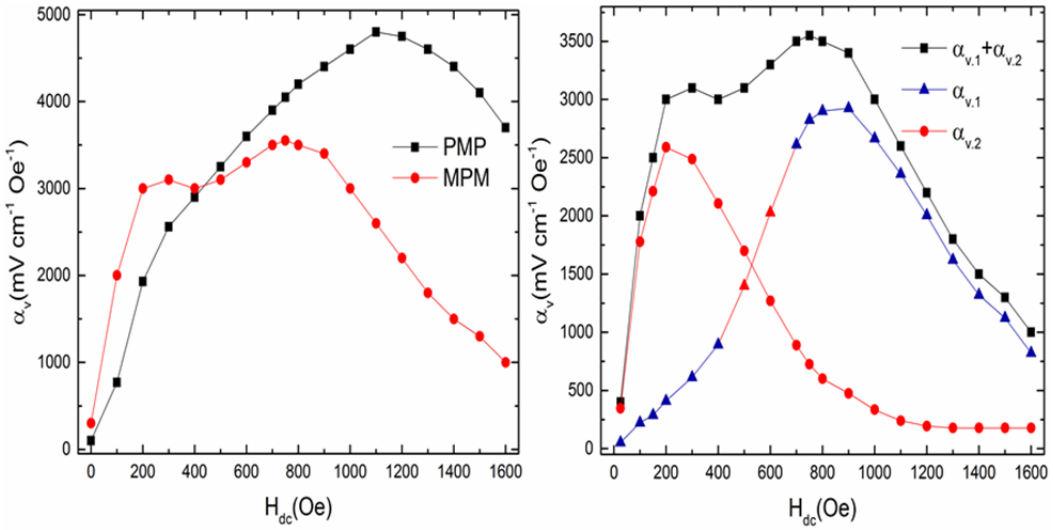

(a) (b)

Figure 3: (a) Magnetoelectric voltage coefficient at 81kHz as a function of H_{dc} for MPM and PMP, (b) Fitted result for magnetoelectric voltage coefficient at 81 kHz as a function of bias magnetic field for MPM.

It needs to be noted that the tread of ME voltage coefficient depending on H_{dc} for MPM was quite different from PMP in Fig. 3(a), and the two peaks were observed in the curve. The unique shape of α_v-H_{dc} curve has not been observed in the tri-layered ME composites with the same length and width as reported in Ref (Li and Chen, 2008).

As shown in Figure 3(b), the α_v-H_{dc} curve could be separated into two curves called α_{v1}-H_{dc} and α_{v2}-H_{dc}, and one normal peak could be observed for each curve. Piezomagnetic coefficient was a three-order tensor, and its components could exhibit different dependence on H_{dc} (Dong et al., 2003). The piezomagnetic coefficient could be written through the coordinates conversion method as follows:

$$d = \begin{bmatrix} d_{11} & 0 & 0 \\ d_{21} & 0 & 0 \\ d_{31} & 0 & 0 \\ 0 & 0 & 0 \\ 0 & 0 & d_{53} \\ 0 & d_{62} & 0 \end{bmatrix}, \begin{bmatrix} \sigma_1 \\ \sigma_2 \\ \sigma_3 \\ \sigma_{12} \\ \sigma_{23} \\ \sigma_{31} \end{bmatrix} = d \begin{bmatrix} H_1 \\ 0 \\ 0 \end{bmatrix} \quad (7)$$

where $d_{21}=d_{31}$, $d_{53}=d_{62}$ and $\sigma_{12}=\sigma_{23}=\sigma_{31}$. Considering the effect of the magnetic field on the strain , $\sigma_1=d_{11}H_1$, $\sigma_2=d_{21}H_1$ and $\sigma_3=d_{31}H_1$could be deduced. It indicated that α_{v1} and α_{v2} in the present work corresponded to the two piezomagnetic coefficient components reaching the maximum values under distinct bias magnetic fields. In the light of the dependence on bias magnetic field for α_{v1} and α_{v2}, the two components of piezomagnetic coefficient could be identified as d_{11} and d_{21}. As shown in Figure 3(b), $\alpha_{v1}+\alpha_{v2}$was consonant with the experimental results observed in Figure 3(b), indicating the reliability for the fitting process.

As already noted in the paper, one peak was observed in the α_v-H_{dc} curve for PMP, and the corresponding H_{dc} was 750 Oe, which was very close to the second peak H_{dc} for MPM. It was deduced that α_{v2} could be attributed to the vibration along the width direction (direction 2 in Fig. 1), for which the d_{21} component contributed to the magnet-electric effect. The peak value of α_{v2} increased significantly with the increasing t_M, while the peak value of α_{v1} decreased significantly with the increasing t_M. Thus, the effects of d_{11} and d_{21} were comparable when t_M equals 0.5mm. As t_M increased or decreased from 0.5mm, one component of piezomagnetic coefficient became not so obvious, and the α_v-H_{dc} curve showed normal shape. Thus the unique shape of α_v-H_{dc} curve in the proposed structure could be attributed to the higher peak value of one piezomagnetic coefficient component, which suppresses the effect of the other component, as shown in Figure 4(a).

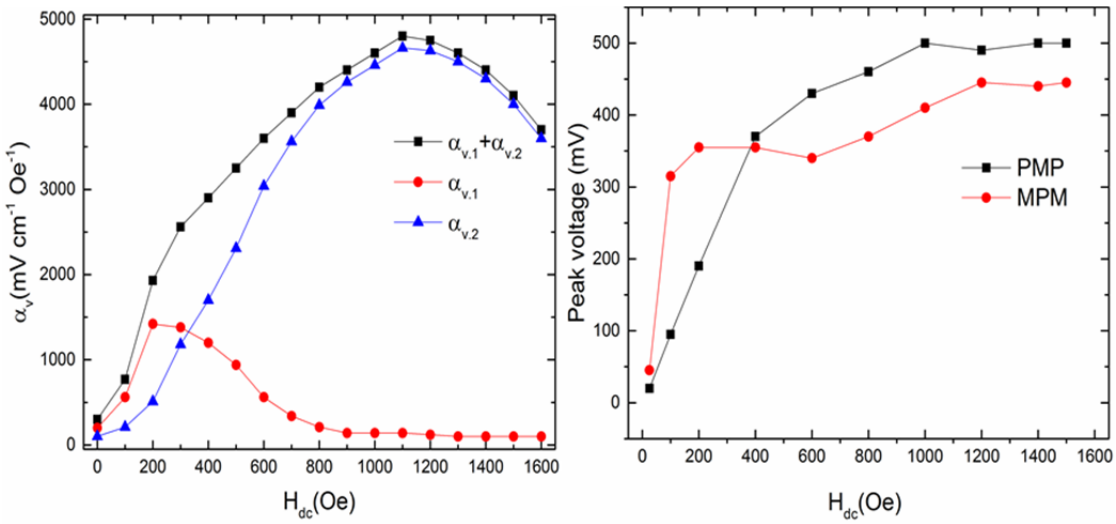

(a) (b)

Figure 4: (a) Fitted result for magnetoelectric voltage coefficient at 81 kHz as a function of bias magnetic field for PMP, (b) The peak voltage for MPM and PMP as a function of H_{dc} at resonance frequency.

The peak voltage output at resonance frequency has attracted significant attention. Figure 4(b) shows the peak voltage for PMP and MPM as a function of H_{dc} at resonance frequency. With the increasing DC bias magnetic field, the peak output for PMP increased rapidly until H_{dc} = 400 Oe, and then slightly increased. Corresponding to this, it could be found that the peak output for MPM increased dramatically up to a value of 360 mV near 200 Oe and then decreased slowly until H_{dc} = 600 Oe and finally slightly increased with the increasing H_{dc}.

The dependence of the peak voltage on H_{dc} originated from the piezomagnetic coefficient dependence on H_{dc}. According to Figure 3(b) and 4(a), the relationship between ME voltage coefficient and piezomagnetic coefficient was analyzed and the peak voltage also depended on α_v-H_{dc} at 81 kHz for MPM and PMP in Figure 3(a). The curves of the first half in Figure 3(a) and 4(b) were similar, in which the peak and ME voltage coefficient increased rapidly and then slightly increased for PMP, where existed a downward process for MPM. However, the curves of the second half in Fig.3(a) and 4(b) were quite different, which mainly resulted from that the peak voltage was the direct proportion to the product of the piezomagnetic coefficient and the effective mechanical quality factor Q_m [Lei and Wang, 2014].

4. Conclusions

ME effects have been investigated for PMP and PMP. Two components of piezomagnetic coefficient were derived and the unique shape observed in α_v-H_{dc} curve at resonance frequency could be attributed to the two

components for Terfenol-D. The peak voltage curves depending on α_V-H_{dc} at resonance frequency for MPM and PMP were quite different, and this was mainly because the peak voltage output was direct proportion to the product of the Q_m and piezomagnetic coefficient. This indicated the possibility of using the PMP or MPM sensor for DC or low level AC magnetic field detection.

Acknowledgement

This work was supported by Ningbo Natural Science Foundation in Zhejiang province, China under Grant No. 2017A610105, the soft science project of Ningbo under Grant No. 2016A10041, and the Public Projects of Zhejiang Province under Grant No. 2015C31150.

References

Bi K., Wang Y.G., Pan D.A., Wu W., 2010, Large magnetoelectric effect in negative magnetostrictive/piezoelectric/positive magnetostrictive laminate composites with two resonance frequencies, Scripta Materialia, 63, 589-592, DOI: 10.1016/j.scriptamat.2010.06.003.

Bi K., Wang Y.G., Pan D.A., Wu W., 2011, Large magnetoelectric effect in mechanically mediated structure of TbFe2, Pb(Zr, Ti)O_3, and nonmagnetic flakes, Applied Physics Letters, 98, 133504, DOI: 10.1063/1.3574004.

Dong S.X., Li J.F., Viehland D., 2003, Giant magneto-electric effect in laminate composites, IEEE Transactions on Ultrasonics, Ferroelectrics, and Frequency Control, 50, 1236-1239.

Lei L., Wang, Y., 2014, Dynamic Magneto-mechanical Behavior of Magnetization-graded Ferromagnetic Materials, Journal of Magnetics, 19, 215-220.

Li L., Chen, X.M., 2008, Magnetoelectric characteristics of a dual-mode magnetostrictive/piezoelectric bilayered composite, Applied Physics Letters, 92, 072903, DOI: 10.1063/1.2840177.

Li L., Chen X.M., Zhou H.Y., 2013, Unique dependence of magnetoelectric voltage coefficient on bias magnetic field in Terfenol-D/Pb(Zr, Ti)O_3 bi-layered composites, Journal of Alloys and Compounds, 553, 86-88, DOI: 10.1016/j.jallcom.2012.11.121.

Li X.Y., Liu J., Zhang N., 2016, Magnetoelectric coupling by acoustic wave guide, Journal of Applied Physics, 119, 134105, DOI: 10.1063/1.4945676.

Liu Y.X., Wan J.G., Liu J.M., Nan C.W., 2003, Effect of magnetic bias field on magnetoelectric coupling in magnetoelectric composites, Journal of Applied Physics, 94, 5118, DOI: 10.1063/1.1613811.

Liu J., Du J.K., Wang J., Yang J.S., 2017, Long thickness-extensional waves in thin film bulk acoustic wave filters affected by interdigital electrodes, Ultrasonics, 75, 226-232, DOI: 10.1016/j.ultras.2016.12.004.

Nan C.W., Bichurin M.I., Dong S.X., Viehland D., Srinivasan G., 2008, Multiferroic magnetoelectric composites: Historical perspective, status, and future directions, Journal of Applied Physics, 103, 031101, DOI: 10.1063/1.2836410.

Wan J.G., Li Z.Y., Wang Y., Zeng M., Wang G.H., Liu J.M., 2005, Strong flexural resonant magnetoelectric effect in Terfenol-D/epoxy-Pb(Zr, Ti)O_3 bilayer, Applied Physics Letters, 86, 202504, DOI: 10.1063/1.1935040.

Wu G.J., Zhang, R., Li, X., Zhang, N., 2011, Resonance magnetoelectric effects in disk-ring (piezoelectric-magnetostrictive) composite structure, Journal of Applied Physics, 110, 124103, DOI: 10.1063/1.3670018.

Zeng M., Or S.W., Chan H.L.W., 2010, Giant magnetoelectric effect in magnet-cymbal-solenoid current-to-voltage conversion device, Journal of Applied Physics, 107, 074509, DOI: 10.1063/1.3372759.